# DIFFRACTION IMAGING IN THREE DIMENSIONS WITH KINEMATIC WAVEFIELD ATTRIBUTES

*S. Dell and D. Gajewski*

**email:** *sergius.delll@zmaw.de*

**keywords:** *3D diffraction imaging*

**ABSTRACT**

*Imaging of diffractions is inherently a 3-D problem. In real geological environments one can not expect diffractors to be located below 2-D profiles. The 3-D effects of diffractors located transverse to the profile line lead to a smeared and less reliable diffraction images. We present a method for 3-D imaging of diffracted events both in the time and depth domain. Our method comprises two steps. At the first step we isolate diffracted events using the kinematic wavefield attributes extracted by the Common-Reflection-Surface method. At the second step we perform migration velocity analysis by evaluating the semblance norm along diffraction traveltimes both in the depth and time domain. Then, we perform Kirchhoff type of poststack migration with estimated velocities to obtain the final diffraction image. The application of the method to synthetic data shows that the proposed method successfully separates diffractions from reflections. The diffraction-only sections allow to determine time and depth migration velocities in the poststack domain which favourably focus diffraction in time and depth.*

## INTRODUCTION

The importance of diffractions in the seismic processing and imaging is more and more recognised. Diffractions are carrier of detailed information about the subsurface in regions of high importance for the reservoir characterisation and exploitation. They provide a naturally and physically justified way to the high-resolution image beyond the classical Rayleigh limit (Khaidukov et al., 2004; Moser and Howard, 2008). Moreover, the diffracted wavefield is determined solely by properties of the medium in a small neighbourhood of the scatterer. Therefore, diffractions can be used to extract detailed velocity information in the nearest vicinity of the potential scatterer providing an illumination usually superior to reflections (Reshef and Landa, 2009).

Imaging of diffractions is still a challenge in the seismic processing because they are inherently of 3-D nature. We need to consider three dimensions if we are interested to correctly image diffractions. Several methods have been developed for this purpose. They are based on the different kinematic behaviour of diffractions in comparison to reflections. Fomel et al. (2006) proposed to isolate diffracted events in the time domain where the smoothness and continuity of local event slopes can be used to separate diffracted and reflected events. Klokov et al. (2011) proposed to isolate diffracted events in the depth domain based on the particular behaviour of the diffractions in the migrated dip-angle domain. For correct velocity models, the diffractions in dip-angle common-image-gathers are flat while reflections exhibit typical 'smiles'. Separation in the depth domain is most suitable for complex media. However, a very well determined velocity model is required. For models with moderate velocity variations, the separation in the time domain is more robust with respect to the quality of the velocity model.

In this paper, we propose an approach for 3-D diffraction imaging in time and depth domain, respectively. Our method is partly based on the Common-Reflection-Surface (CRS) technique. We use the CRS technique to extract the kinematic wavefield attributes. We employ these attributes to identify and isolate

diffracted events in the time domain. The events separation is based on a simultaneous application of the CRS-based diffraction operator and a reflection attenuation algorithm. The attenuation algorithm is an extension of the 2-D diffraction filter (Dell and Gajewski, 2011).

In the next section, we present our concept to isolate seismic events based on their kinematic behaviour in the time domain.

## ISOLATION OF DIFFRACTED EVENTS

We use the CRS approach to identify the diffracted events (see about CRS method, e.g., in Jäger et al., 2001). According to the CRS theory, a diffractor is associated with a reflector segment with an infinite curvature and an indefinite orientation (Mann, 2002). Also for diffractions any direction describes a possible zero-offset ray along which the Normal-Incident-Point (NIP) wave (Hubral, 1983) and normal wave can be considered. This implies component-wise equality of matrices containing both wavefront curvatures, $\mathbf{K}_N = \mathbf{K}_{NIP}$. Here $\mathbf{K}_{NIP}$ is the matrix of curvatures of the NIP-wave and $\mathbf{K}_N$ is the matrix of curvatures of the normal wave. Both matrices represent kinematic wavefield attributes since they contain kinematic information of the propagation of the normal ray (Höcht, 2002). The CRS operator for a diffracted event is given as

$$t(\mathbf{m},\mathbf{h})^2 = \left(t_0 + 2\,\Delta\mathbf{m}^T\mathbf{p}_m\right)^2 + \frac{2t_0}{v_0}\left(\mathbf{h}^T\mathbf{H}\mathbf{K}_{NIP}\mathbf{H}^T\mathbf{h} + \Delta\mathbf{m}^T\mathbf{H}\mathbf{K}_{NIP}\mathbf{H}^T\Delta\mathbf{m}\right), \tag{1}$$

where $\mathbf{h}$ is half-offset vector, $\Delta\mathbf{m}$ is the midpoint displacement vector, $t_0$ corresponds to the vertical zero-offset two-way traveltime, and $v_0$ is the surface velocity. The vector $\mathbf{p}_m$ is the horizontal component of the slowness vector of the central ray and contains of an emergence angle and a dip angle. $\mathbf{H}$ is the transformation matrix from ray centred to the general coordinate system.

The equality $\mathbf{K}_N = \mathbf{K}_{NIP}$ can be used to identify diffracted events. Moreover, in the principle system the matrix $\mathbf{K}_{NIP}$ has two non-zero diagonal elements. These diagonal elements are the principal curvatures of the wavefront and coincide for a diffracted event. Therefore, the 2-D diffraction filter proposed in Dell and Gajewski (2011) can be extended to three dimensions without significant modifications. For the 3-D case, we suggest to use following function as a threshold function:

$$T_F = e^{-\frac{|Kn_{00} - Knip_{00}|}{|Kn_{00} + Knip_{00}|}}, \tag{2}$$

where $Kn_{00}$ is the upper-right diagonal element of the curvature matrix of the normal wave, $\mathbf{K}_N$, and $Knip_{00}$ is the upper-right diagonal element of the curvature matrix of the NIP-wave, $\mathbf{K}_{NIP}$, respectively. This function is about one for $Knip_{00}$ close to $Kn_{00}$ and rather small if $Knip_{00}$ and $Kn_{00}$ differ.

To isolate the diffracted events, we apply the CRS-based diffraction operator given by equation (1) to the prestack data if the threshold function, $T_F$, is above a determined value and do not stack in the opposite case. The application of the separation technique will exclude reflected events in the stacked section because they have a lower value of $T_F$. In the contrast, diffracted events will be coherently stacked because they have a higher value of $T_F$. The final stacked section will then contain predominantly diffraction energy.

In the next section, we describe how to build velocity models fast and effectively by exploiting diffractions in the poststack domain.

## IMAGING DIFFRACTED EVENTS

The isolated diffracted events allow to identify the presence of small heterogeneities, truncations, faults. However, to reliable interpret such subsurface features caused by diffractions, the letter ones should be properly imaged. An inherent part of the imaging is therefore a migration velocity analysis which should be tuned to diffractions. The velocity analysis presented in this paper is based on a coherence analysis for diffraction traveltimes. We use the semblance norm as a measure of the coherence (Taner and Koehler, 1969).

### Time domain

In the time domain, the diffraction traveltimes are computed by the double-square-root (DSR) equation which for $\mathbf{h} = 0$ simplifies to

$$t_D = \sqrt{t_0^2 + \frac{\mathbf{m}^2}{v_{migr}^2}}\,, \tag{3}$$

where $\mathbf{m}$ is midpoint vector and $v_{migr}$ is time-migration velocity. To estimate time-migration velocity, we perform a velocity scan from low to high velocities evaluating the semblance value for each sample in the stacked section. The output is a coherence map which is suitable for picking time migration velocities.

We assume for the time-migration velocity analysis presented here an isotropic medium. However, we can straightforward expand the velocity analysis to anisotropic media by replacing the conventional DSR equation with the DSR equation as formulated in Alkhalifah and Tsvankin (1995). In this case, one-term velocity analysis will became a bispectral analysis whereby semblance values will be computed for each sample as a function of the time-migration velocity $v_{migr}$ and an effective anelliptical parameter $\eta_{eff}$.

### Depth domain

To find traveltimes of a diffractor in the depth domain, we suggest to calculate them analytically instead of using more involved ray-tracing. We will consider two cases: a subsurface with a constant velocity and a subsurface with a constant gradient of velocities. In both cases there is an analytical solution for traveltimes. For more general velocity models however one would have to use ray-tracing approach to calculate diffraction traveltimes.

### Medium with constant velocity

The velocity analysis here will provide an effective velocity for each depth position which can be used for depth migration. In these media, the ray paths are straight line so that traveltimes can be directly computed using the Pythagoras theorem as reads

$$t_D = \frac{1}{v}\sqrt{x^2 + y^2 + z^2} \tag{4}$$

where $v$ is the migration velocity to be determined. To find the velocity $v$ we discretise the subsurface. For each grid point we calculate the diffraction traveltimes using equation (4) for different values of velocities and evaluate the corresponding semblance norm. The output is a coherence map as in the time domain.

### Medium with constant velocity gradient

The velocity analysis in media with constant vertical velocity gradient will provide a smoothed velocity model which can be used for depth migration of both reflected and diffracted events. To calculate diffracted traveltimes, we use an analytical solution of the Kirchhoff integral for a vertical inhomogeneous medium (Martins et al., 1997) which we adapt to the poststack domain. We consider the velocity distribution is controlled by following law

$$v(z) = v_0 + \gamma z\,, \tag{5}$$

where $\gamma$ is a constant velocity gradient, and $v_0$ is the surface velocity. Once the subsurface is discretized, the diffracted traveltimes for a depth point can be obtained as

$$t(x, y, z) = \frac{2}{\gamma}\ln\left(1 + \frac{1 + \sqrt{1 + 2B}}{B}\right)\,, \tag{6}$$

where

$$B = \frac{2vv_0}{\gamma^2(x^2 + y^2 + z^2)}\,.$$

Similarly to the time-domain, we perform a scan from low to high gradient. This means, for every depth point we compute diffraction traveltimes using equation (6) evaluating the semblance value for different gradient values. The output is a gradient panel suitable for picking. The gradient, that corresponds to the maximum semblance, is then used to calculate the velocity distribution according equation (5).

## SYNTHETIC EXAMPLE

In this section, we show an application of the presented method for diffraction imaging to synthetic data. Figure 1 shows the model which consists of three homogeneous layers and a sphere placed at 2 km depth in the third layer. The radius of the sphere is 100 meter. The velocity in the first layer is 1500 $m/s$. The velocity in the second layer is 1700 $m/s$. The velocity in the third layer is 2000 $m/s$. The seismograms were generated using the NORSAR 3D ray-tracing. The dominant frequency is 20 Hz. Also some band-limited noise of the Gauss type is added. The CRS stacked section containing 13 crosslines is shown in Figure 2. We determine the CRS attributes using offsets up to 200 m in both X and Y direction since the CRS operator is a single-square root operator thus an approximation valid for short offsets. We determined the value for the threshold function as 0.7. We chose the quite low value of the threshold function in order to properly separate seismic events far away from the diffraction apex. This type of seismic events suffers from a fact that a proper determination of the $\mathbf{K}_N$ attribute is not possible near data boundaries. The lower value of threshold function $T_F$ used for filtering causes that reflections pass the attenuation process. The CRS stacked section after application of our method is presented in Figure 3 and confirms the above conclusion. The reflections are well attenuated. The present residual reflections are, as predicted, close to the data boundaries and due to aperture effects.

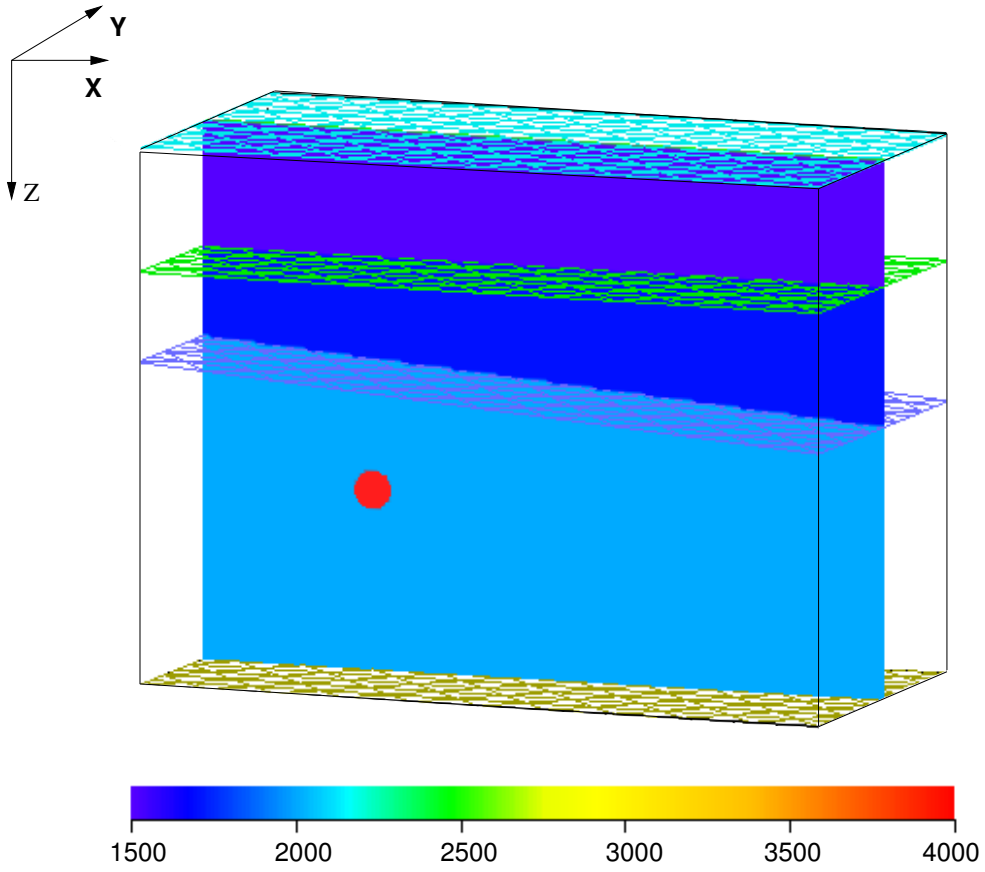


**Figure 1:** 3-D model. The model consists of two layers, a flat one and inclined one, and a sphere placed at the 2 km depth. The radius of the sphere is 100 meter.

We use the diffraction-only data for migration velocity analysis. At first, time migration velocity analysis is applied to the diffraction section. Figure 4a shows the time-migration velocity panel for a CMP

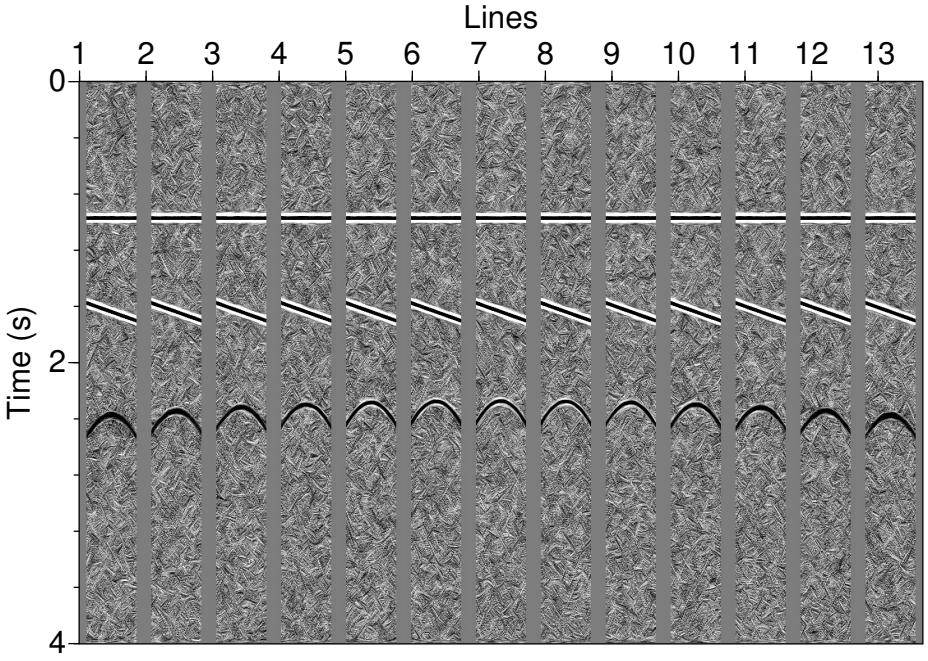


**Figure 2:** CRS stacked section of diffracted and reflected events. For parameter searches we used shot offset apertures. We can see, that for the crossline directly above the diffractor, zero-offset CRS stack provides a very good approximation of diffraction response.

which is directly above the diffraction apex. The high value of semblance is almost one and indicates that the velocity is determined correctly. Note that a semblance based analysis is usually influenced by the poor signal-to-noise ratio. However, the S/N ratio is improved in the poststack domain therefore more reliable velocities can be extracted. Figure 4b shows a semblance plot as a function of lateral position, X coordinate, for the correct time-migration velocity. We observe a semblance maximum at the correct special position of the diffraction apex. Also the lateral focusing is very good, i.e., the proposed velocity analysis provides both the correct time-migration velocity and the spacial position of the diffraction apex. With the estimated velocity model we perform poststack Kirchhoff time migration. Figure 5 shows the time-migrated image of the diffraction-only data. The diffraction is well focused validating the correctness of the estimated time-migration velocities.

Also depth migration velocity analysis is applied to the diffraction-only data. First, we apply scans for effective medium-velocities. Figure 6 shows the effective-velocity panel for a CMP which is located directly above the diffractor location. Figure 8 shows the depth-migrated image of the isolated diffracted events. The diffraction is well focused. However, we observe that the residual reflection is still present similarly to the time-migrated section. Although the residual reflection is focused in the CRS stacked section it is very smeared in the migrated sections. The reason for this may be a contribution of boundary effects because of the limited operator size and the end of the reflector boundary (Hertweck et al., 2005). In this case, the migration stack does not sum up all the data necessary for complete destructive interference and, as a consequence, migration artifacts appear resulting in a smeared reflection image. Figure 7 shows the gradient panel for a CMP which is directly above the diffractor position. Also here the semblance value is quite high. The smoothed depth velocity model can be calculated using equation (5). These velocities can be used as an initial velocity model for depth migration of all seismic events.

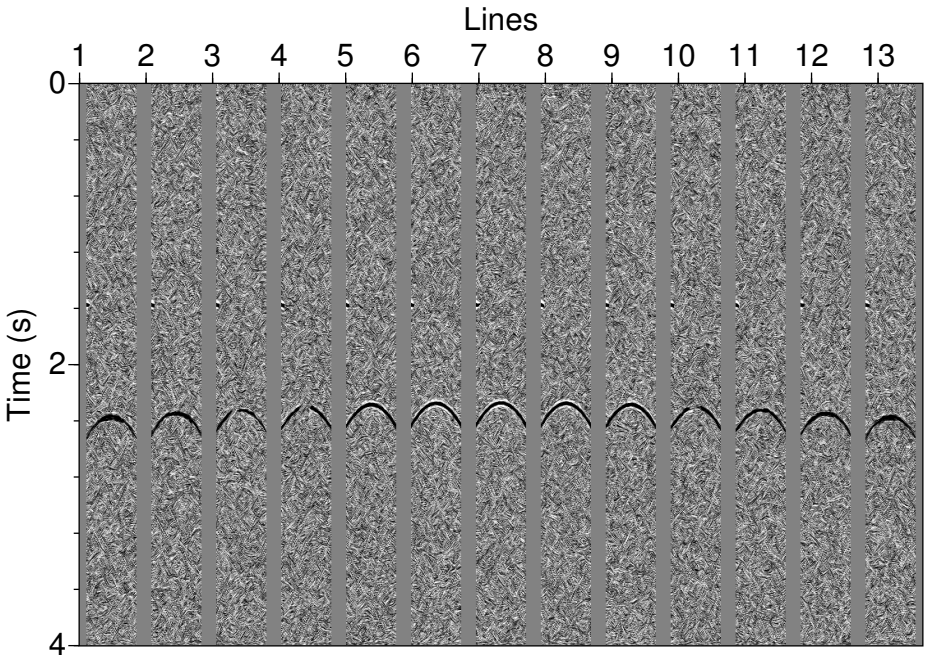


**Figure 3:** Stacked section after the application of the separation algorithm. The reflected events are well attenuated. However, some parts of residual reflections are still present. We explain their presence due to complexity of the proper attribute estimation near the section border.

## DISCUSSION AND CONCLUSIONS

We have presented a method to image diffractions in three dimensions. The novelty of the method is the separation of diffracted events in three dimensions using kinematic wavefield attributes and migration velocity analysis using diffraction traveltimes. The first step in our approach is the attenuation of reflected events by a simultaneous application of the CRS-based diffraction operator and a diffraction filter.

The isolated diffracted events we used for a poststack migration velocity analysis. The velocity analysis consists of a velocity scan and the evaluation of the corresponding semblance norm for each sample in the time domain or grid point in the depth domain, respectively. In the poststack domain, the data are reduced and a good S/N ratio is present. The computational efficiency of analytical traveltime calculations coupled with the speed and low cost of current high performance computing techniques allow a very fast and robust initial depth-migration velocity analysis.

Application to synthetic data demonstrates that the presented method leads to focused images of diffracted events.

## ACKNOWLEDGMENTS

The authors would like to thank the sponsors of WIT consortium for their support. We also thank NORSAR Innovation AS for kindly permition to use NORSAR ray tracing package. We are grateful to AGG Hamburg for helpful discussions.

## REFERENCES

Alkhalifah, T. and Tsvankin, I. (1995). Velocity analysis for transversely isotropic media. *Geophysics*, 60:1550–1566.

Dell, S. and Gajewski, D. (2011). Common-Reflection-Surface-based workflow for diffraction imaging. *Geophysics*, page accepted.

Fomel, S., Landa, E., and Taner, M. T. (2006). Posstack velocity analysis by separation and imaging of seismic diffractions. *Geophysics*, 72:no. 6, U89–U94.

Hertweck, T., Jäger, C., Goertz, A., and Schleicher, J. (2005). Aperture effects in 2.5-D Kirchoff migration: A geometrical explanation. *Geophysics*, 68(5):1673–1684.

Höcht, G. (2002). *Traveltime approximations for 2D and 3D media and kinematic wavefield attributes*. PhD thesis, University of Karlsruhe.

Hubral, P. (1983). Computing true amplitude reflections in a laterally inhomogeneous earth. *Geophysics*, 48:1051–1062.

Jäger, R., Mann, J., Höcht, G., and Hubral, P. (2001). Common-reflection-surface stack: Image and attributes. *Geophysics*, 66:97–109.

Khaidukov, V., Landa, E., and Moser, T. J. (2004). Diffraction imaging by focusing-defocusing: An outlook on seismic superresolution. *Geophysics*, 69:1478–1490.

Klokov, A., Baina, R., and Landa, E. (2011). Point and edge diffractions in three dimensions. In *73th Conference and Technical Exhibition, EAGE*, page B023. Extended Abstracts.

Mann, J. (2002). *Extensions and Applications of the Common-Reflection-Surface Stack Method*. Logos Verlag Berlin.

Martins, J. L., Schleicher, J., Tygel, M., and Santos, L. (1997). 2.5-D True-amplitude Migration and Demigration. *Journal of Seismic Exploration*, 6:159–180.

Moser, T. J. and Howard, C. B. (2008). Diffraction imaging in depth. *Geophysical Prospecting*, 56:627–641.

Reshef, M. and Landa, E. (2009). Post-stack velocity analysis in the dip-angle domain using diffractions. *Geophysical Prospecting*, 57:811–821.

Taner, M. and Koehler, F. (1969). Velocity-spectra digital computer derivation and applications of velocity functions. *Geophysics*, 34:859–881.

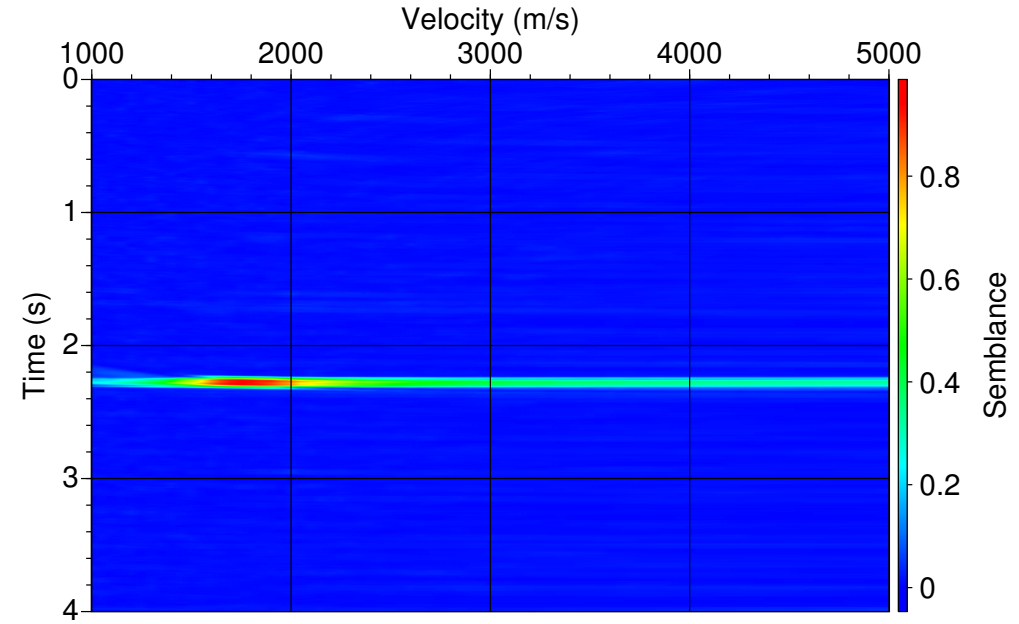


(a)

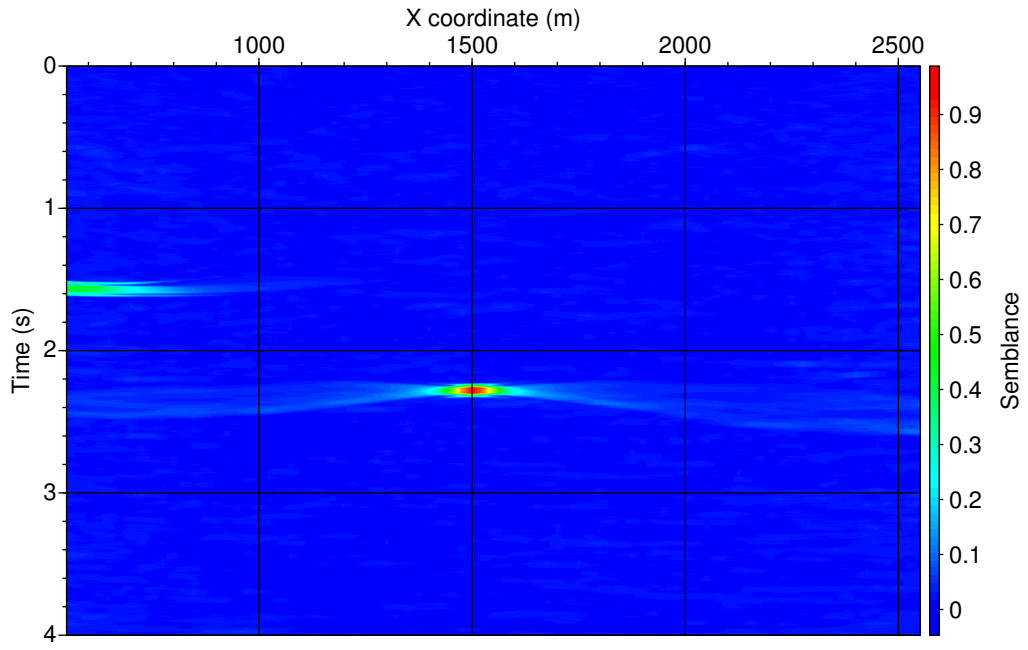


(b)

**Figure 4:** Results of time-migration velocity analysis. (a) Time-migration velocity panel. The velocity panel is chosen for a CMP which is directly above the diffraction apex. The high value of semblance indicates the velocity is correctly determined. (b) Semblance plot as a function of lateral position, X coordinate, for the correct time-migration velocity. The semblance maximum is at the correct special position of the diffraction apex.

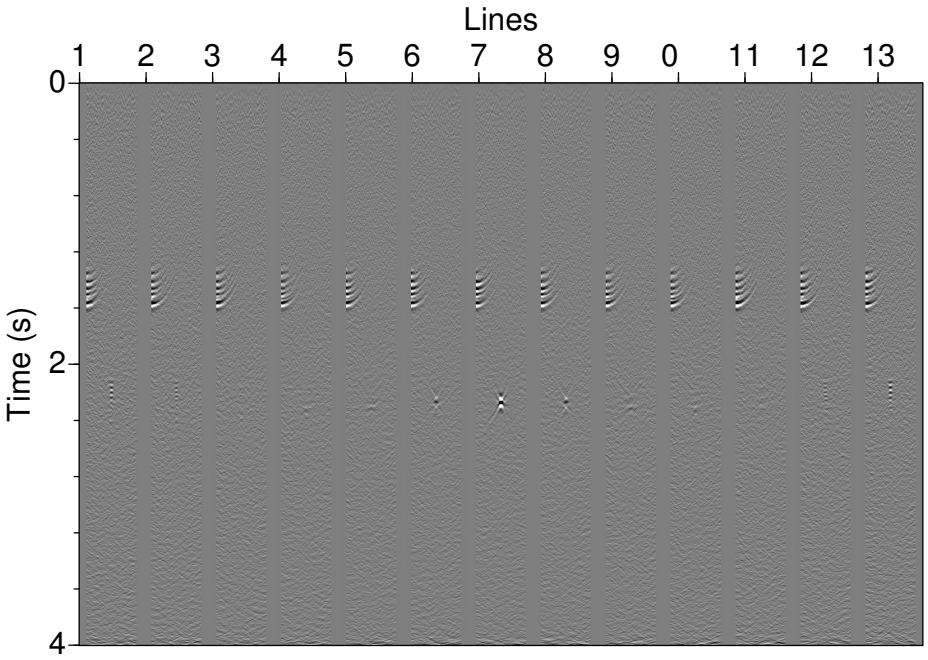


**Figure 5:** Time-migrated section of diffraction-only data. We used the estimated time-migration velocities to perform 3-D poststack Kirchhoff time-migration. The diffraction is well focused to its apex that confirms our time-migration velocity analysis. Artefacts in image caused by residual reflected events are due to aperture effects.

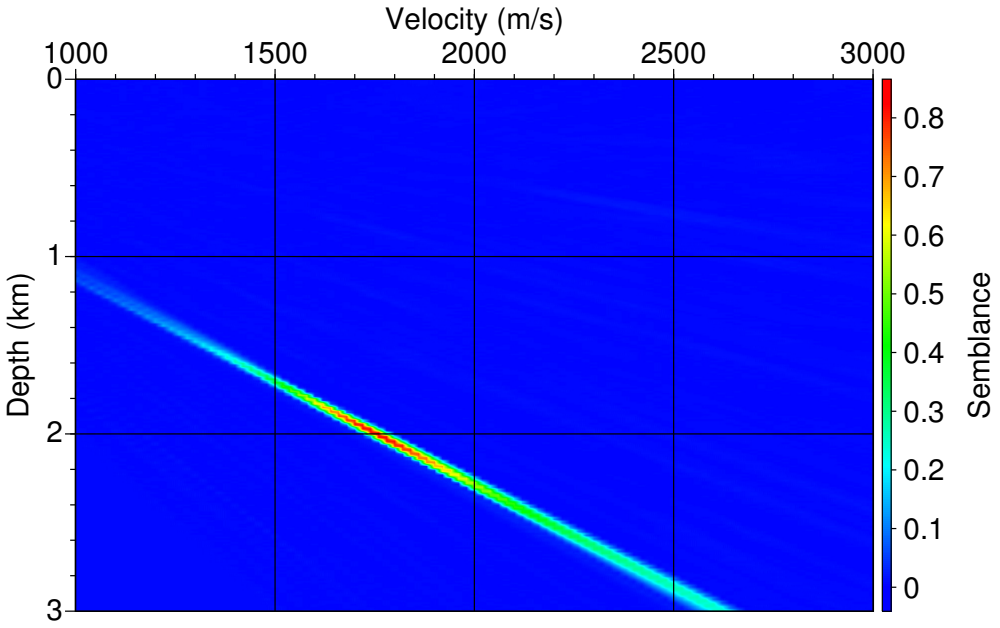


**Figure 6:** Depth-migration velocity panel for a CMP which is directly above the diffractor location. The estimated depth velocity is an effective medium velocity. The high value of semblance indicates that the calculated traveltimes match seismograms well.

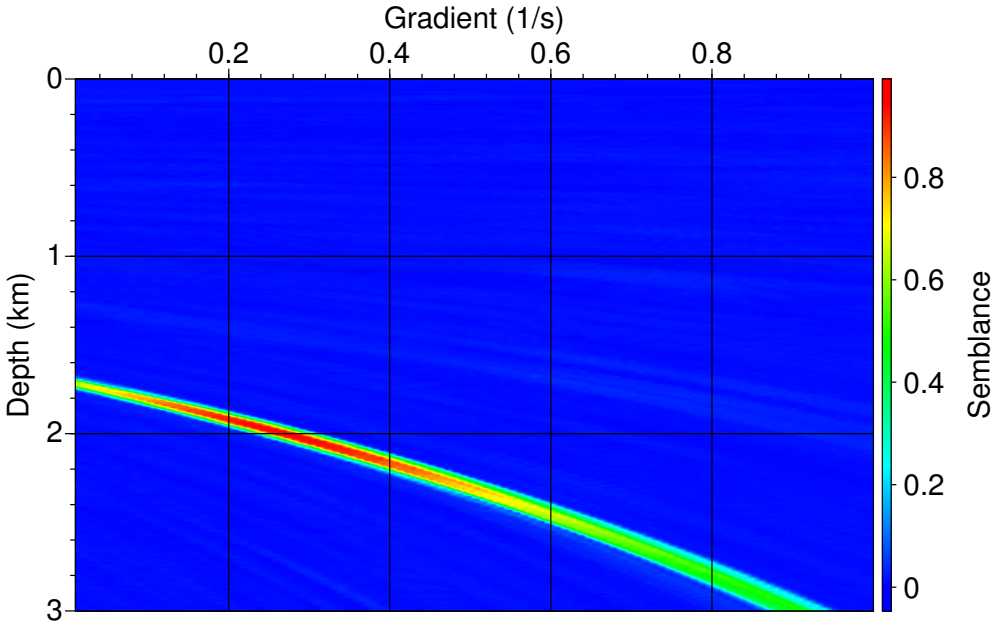


**Figure 7:** Gradient panel. The estimated gradients can be used to calculate a smooth depth velocity model. These velocities can be used as an initial velocity model for poststack Kirchhoff depth migration of both reflected and diffracted events.

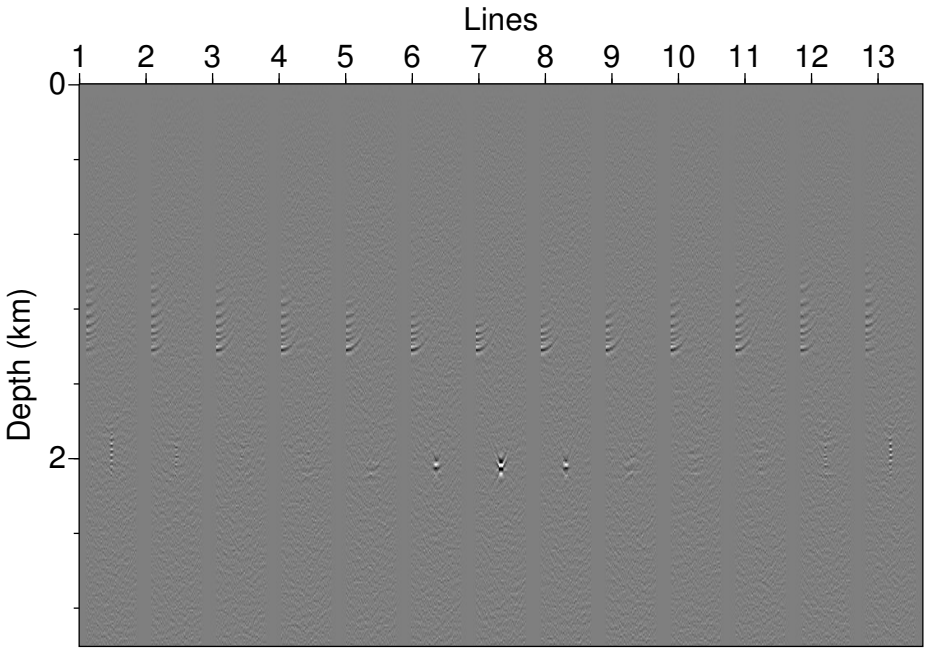


**Figure 8:** Depth-migrated section of diffraction-only data. We used the estimated effective velocities for 3-D poststack Kirchhoff depth-migration with a constant velocity. The diffraction is well and correct focused to its spatial position. Artefacts in image caused by residual reflected events are due to aperture effects.